



Study on Effect of Boundary Conditions in Transient Dynamic Stress Analysis of Thick Cylindrical Shells under Internal Moving Pressure

H. Ramezani, M. Mirzaei*

Department of Mechanical Engineering, Tarbiat Modares University, Tehran, Iran

ABSTRACT: This study presents a new analytic solution for transient elasto-dynamic structural response of cylindrical shells to internal moving load under different boundary conditions. The equations of motion of a thick shell are used and the effects of transverse shear and rotary inertia are considered. The general form of the presented formulations and the solution method are applicable to many theoretical and practical problems. However, the formulation is adjusted for gaseous detonation loading. The pressure history of the detonation loading, which consists of a shock wave and a reaction zone, is represented by an exponential approximation to the Taylor-Zeldovich model. The presented analytic solution is validated through comparison with the available experimental data from the literature and finite element simulations. Representative analyses are carried out for an experimental detonation tube subjected to different boundary conditions including simply-supported, clamped-clamped, and clamped-free. Results show that obtained vibrational behavior can be highly affected by the types of boundary conditions especially for locations near the end of the tube, where the interference between the forward traveling waves and the reflected waves is quite significant.

Review History:

Received: 26 December 2016
Revised: 16 May 2016
Accepted: 21 May 2016
Available Online: 7 June 2017

Keywords:

Cylindrical shell
Transient dynamic loading
Structural response
Boundary conditions.

1- Introduction

The structural response of cylindrical shells to internal moving pressures is part of broader problems of design and analysis of pressure vessels for containment of internal gaseous explosions. There have been several studies on the analysis of the vibrational behavior of cylindrical tubes under moving pressures. The first comprehensive theories were developed by Tang [1]. The model presented by Tang included the effects of transverse shear and rotary inertia and presented steady state solutions for an infinite tube. The experimental, analytical, and numerical studies carried out by Beltman and Shepherd [2] showed that the true characteristics of the response for finite tubes can only be revealed through transient models. They made two major simplifications to the governing equations of the Tang's model and also dropped the effects of transverse shear and rotary inertia to obtain a tractable transient formulation. They reported the structural responses of simply-supported and clamped tubes to the Taylor-Zeldovich pressure profile. Mirzaei et. al. [3-7] modified the original Tang's formulation and developed new transient analytic models for simply-supported finite tubes, in which all the essential terms in the governing equation, including transverse shear and rotary inertia, were preserved. In the current study, an analytical solution for the transient elastodynamic response of thick cylindrical shell, with different boundary conditions, to moving pressure is presented. The boundary conditions are simply-supported, clamped-clamped, and clamped-free. The presented analytic solutions are validated by comparison with the available experimental data and also finite element simulations.

2- Description of the Problem

The elastodynamic behavior of a circular cylindrical thick shell of finite length L , main radius R , and thickness h , which is subjected to internal moving pressure, is modelled and the variation of the hoop strain with time is calculated. From the structural point of view, the tube experiences a traveling internal axisymmetric load along the axial direction that produces transient dynamic deformations. The formulation of the transient loading functions comprises of two phases as follows;

$$p(x,t) = \begin{cases} P_1 + \left(P_3 - P_1 + (P_2 - P_3)e^{\frac{x-Vt_1}{VT}} \right) H(Vt_1 - x) & 0 \leq t_1 < \frac{L}{V} \\ P_3 + (P_2 - P_3)e^{\frac{x-Vt_2-L}{VT}} & 0 \leq t_2 < \infty \end{cases} \quad (1)$$

where P_1 , P_2 , P_3 , T , $H()$, and V are the initial pressure of the gas mixture, peak pressure, final pressure, exponential decay factor, Heaviside function, and velocity of moving load, respectively. The radial displacement of tube, w , is the combination of radial displacement due to bending, w_b , and radial displacement due to shearing, w_s .

The following governing equation of the bending radial displacement can be developed for modeling the analytical transient behavior of the tube [7].

$$\frac{\partial^4 w_b}{\partial x^4} + B_1 \frac{\partial^4 w_b}{\partial t^2 \partial x^2} + B_2 \frac{\partial^2 w_b}{\partial t^2} + B_3 \frac{\partial^2 w_b}{\partial x^2} + B_4 w_b = \frac{144 F(x,t)}{h^3} \quad (2)$$

Corresponding author, E-mail: mmirzaei@modares.ac.ir

where

$$B_1 = -\left(\frac{1}{V_d^2} + \frac{1}{V_s^2}\right), B_2 = \frac{12}{h^2 V_d^2} \left(1 + \beta^2 \frac{V_d^2}{V_s^2}\right), \quad (3)$$

$$B_3 = -\frac{12\beta^2(1 - \beta^2)}{h^2} \frac{V_d^2}{V_s^2}, B_4 = \frac{144\beta^2}{h^4}.$$

and

$$V_d = \sqrt{\frac{E}{\rho(1-\nu^2)}}, V_s = \sqrt{\frac{\kappa G}{\rho}}, \beta = \frac{h}{\sqrt{12}R}. \quad (4)$$

In Eq. (2) we have:

$$F(x,t) = \begin{cases} \Lambda_1 + \left(\Lambda_3 - \Lambda_1 + (\Lambda_2 - \Lambda_3)e^{\frac{x-Vt}{VT}}\right)H(Vt_1 - x) & 0 \leq t_1 \leq L/V \\ \Lambda_3 + (\Lambda_2 - \Lambda_3)e^{\frac{x-Vt_2-L}{VT}} & 0 \leq t_2 \leq \infty \end{cases} \quad (5)$$

where

$$\Lambda_j = \beta^2(1 - \nu^2) \left(1 - \frac{h}{2R}\right) \frac{(P_j - P_{ext})R^2}{Eh^2}, \quad j = 1, 2, 3. \quad (6)$$

3- Formulation of the Problem

Radial displacement can be described as:

$$w(x,t) = \sum_{n=1}^{\infty} \phi_n(x) \eta_n(t) \quad (7)$$

where mode shapes, $\phi_n(x)$, can be considered as [8]

a. for simply-supported

$$\phi_n(x) = \sqrt{\frac{2}{L}} \sin(\lambda_n x); \lambda_n = \frac{n\pi}{L} \quad (8)$$

b. for clamped-clamped

$$\phi_n(x) = \sqrt{\frac{1}{L}} \left(\varphi_1(\lambda_n x) - \frac{\varphi_1(\lambda_n L)}{\varphi_2(\lambda_n L)} \varphi_2(\lambda_n x) \right) \quad (9)$$

c. for clamped-free

$$\phi_n(x) = \sqrt{\frac{1}{L}} \left(\varphi_1(\lambda_n x) - \frac{\varphi_3(\lambda_n L)}{\varphi_4(\lambda_n L)} \varphi_2(\lambda_n x) \right) \quad (10)$$

In Eqs. (9) and (10) we have:

$$\begin{aligned} \varphi_1(\lambda_n x) &= \cosh(\lambda_n x) - \cos(\lambda_n x) \\ \varphi_2(\lambda_n x) &= \sinh(\lambda_n x) - \sin(\lambda_n x) \\ \varphi_3(\lambda_n x) &= \cosh(\lambda_n x) + \cos(\lambda_n x) \\ \varphi_4(\lambda_n x) &= \sinh(\lambda_n x) + \sin(\lambda_n x) \end{aligned} \quad (11)$$

In Eqs. (9) and (10), the eigenvalues (λ_n) can be calculated from $\cosh(\lambda_n x)\cos(\lambda_n x) - 1 = 0$ and $\cosh(\lambda_n x)\cos(\lambda_n x) + 1 = 0$, respectively.

By using Eqs. (8) to (10), the radial displacements can be obtained as:

$$w(x,t) = \begin{cases} \sum_{n=1}^{n^*} \eta_n(t_1) \left(\phi_n(x) - \frac{h^2}{12} \left(\frac{V_d^2 - V^2}{V_s^2} \right) \frac{\partial^2 \phi_n(x)}{\partial x^2} \right), & t < \frac{L}{V} \\ \sum_{n=1}^{n^*} \eta_n(t_2) \left(\phi_n(x) - \frac{h^2}{12} \left(\frac{V_d^2 - V^2}{V_s^2} \right) \frac{\partial^2 \phi_n(x)}{\partial x^2} \right), & t \geq \frac{L}{V} \end{cases} \quad (12)$$

The rationale for development of the solution in closed form and the definition of n^* can be found in [5-7].

In the above equations we have:

$$\eta_n(t_1) = \frac{1}{Y_n \omega_n^2} \int_0^{\frac{L}{V}} \frac{144}{h^3} \Lambda_1 \phi_n(x) dx + \frac{1}{Y_n \omega_n} \int_0^{\frac{L}{V}} \int_0^{\frac{L}{V}-\tau} \frac{144}{h^3} \left(\Lambda_3 - \Lambda_1 + (\Lambda_2 - \Lambda_3) e^{\frac{x-V\tau}{VT}} \right) \phi_n(x) \sin(\omega_n(t_1 - \tau)) dx d\tau \quad (13)$$

and

$$\eta_n(t_2) = \left(\eta_n \left(\frac{L}{V} \right) \right)_{phase1} - \frac{\Lambda_3}{Y_n \lambda_n \omega_n^2} (1 - \cos(\lambda_n L)) \cos(\omega_n t_2) + \left(\frac{d\eta_n \left(\frac{L}{V} \right)}{dt_1} \right)_{phase1} \frac{\sin(\omega_n t_2)}{\omega_n} + \frac{1}{Y_n \omega_n^2} \int_0^{\frac{L}{V}} \frac{144}{h^3} \Lambda_3 \phi_n(x) dx + \frac{1}{Y_n \omega_n} \int_0^{\frac{L}{V}} \int_0^{\frac{L}{V}-L} \frac{144}{h^3} (\Lambda_2 - \Lambda_3) e^{\frac{x-V\tau-L}{VT}} \phi_n(x) \sin(\omega_n(t_2 - \tau)) dx d\tau \quad (14)$$

where

$$Y_n = \int_0^L \left(B_1 \frac{\partial^2 \phi_n(x)}{\partial x^2} + B_2 \phi_n(x) \right) \phi_n(x) dx \quad (15)$$

4- Numerical Simulation

To verify the proposed analytical solution, a series of complementary Finite Element (FE) simulations were carried out using the ABAQUS/CAE commercial package. The FE model was built using 10000 axisymmetric elements (with 1000 and 10 elements in the longitudinal and radial directions respectively). These numbers were obtained from a thorough convergence study on the accuracy and precision of the results for a simple-supported tube through comparisons with the available experimental data, which means that all the parameters of the FE model were rigorously calibrated before the application of other boundary conditions.

5- Results

This section starts with a comparison between the results obtained from the presented analytical formulation and the reported results for a simply-supported tube [2]. Fig. 1 depicts this comparison. The hoop strain histories are for gauges 5 and 10 which are located at 0.79 m and 2.195 m from the entrance of the tube, respectively. The load speeds are 1478.8, and 1699.7 m/s, for which the maximum pressures are 1.35, and 1.7 MPa, respectively. Exponential decay factor T , is taken $4.34e-4$ s. The geometrical and mechanical properties of the tube are listed in Table 1. Shear correction factor is taken 5/6. As shown in Fig. 1, the comparison demonstrates a very good

Table 1. Geometrical and mechanical properties of the tube

L m	R cm	H cm	E GPa	ρ kg/m3	ν
2.38	15.24	2.54	193	8000	0.23

agreement between the analytical results and experiment. The development of the precursors and the modulation of the oscillations of the main signal are predicted by the transient analytic models. In general the predicted wave amplitudes are stronger than the experimental results while the frequencies and modulations of oscillations are essentially similar. This effect, which is more pronounced for gage 10, can be attributed to the damping effects of the tube supports on the reflected structural waves. In practice, these supports can deviate from the ideal simple-support conditions.

Fig. 2 shows a comparison between analytical results and FE simulations for a clamped-free tube. The excellent agreement between the two sets of results, which are obtained at two different locations and for different load speeds, indicate the

accuracy and precision of the presented analytic solution for prediction of the structural response of cylindrical tubes to internal moving pressure.

6- Conclusion

The results of this study showed the accuracy of the proposed analytic solution. It was also shown that the vibrational behavior can be highly affected by the type of boundary conditions, especially for locations where the interference between the forward waves and the reflected waves is quite significant.

References

[1] S. Tang, Dynamic response of a tube under moving pressure, in: Proceedings of the American Society of Civil Engineers, Engineering Mechanics Division, Vol. 5, pp. 97–122, 1965.
 [2] W. M. Beltman, J. E. Shepherd, Linear elastic response of tubes to internal detonation loading, *J. Sound Vib.*, Vol. 252, pp. 617–655, 2002.
 [3] M. Mirzaei, K. Mazaheri, H. Biglari, Analytical modeling of the elastic response of tubes to internal detonation

loading, *Int. J. Press. Vessels Piping*, Vol. 82, No. 12, pp. 883–895, 2005.
 [4] M. Mirzaei, H. Biglari, M. Salavatian, Analytical and numerical modeling of the transient elasto-dynamic response of a cylindrical tube to internal detonation loading, *Int. J. Press. Vessels Piping*, Vol. 83, No 7, pp. 531–539, 2006.
 [5] Mirzaei, On amplification of stress waves in cylindrical tubes under internal dynamic pressures, *Int. J. Mech. Sci.*, Vol. 50, No. 8, pp. 1292–1303, 2008.
 [6] M. Mirzaei, Vibrational response of thin tubes to sequential moving pressures, *Int. J. Mech. Sci.*, Vol. 59, pp. 44–54, 2012.
 [7] M. Mirzaei, M. J. Torkaman Asadi, R. Akbari, On vibrational behavior of pulse detonation engine tubes, *Aerospace Science and Technology*, Vol. 47, pp. 177–190, 2015.
 [8] W. Soedel, *Vibrations of Shells and Plates*, 3rd Edition, Marcel Dekker Inc., New York, USA, 2004.

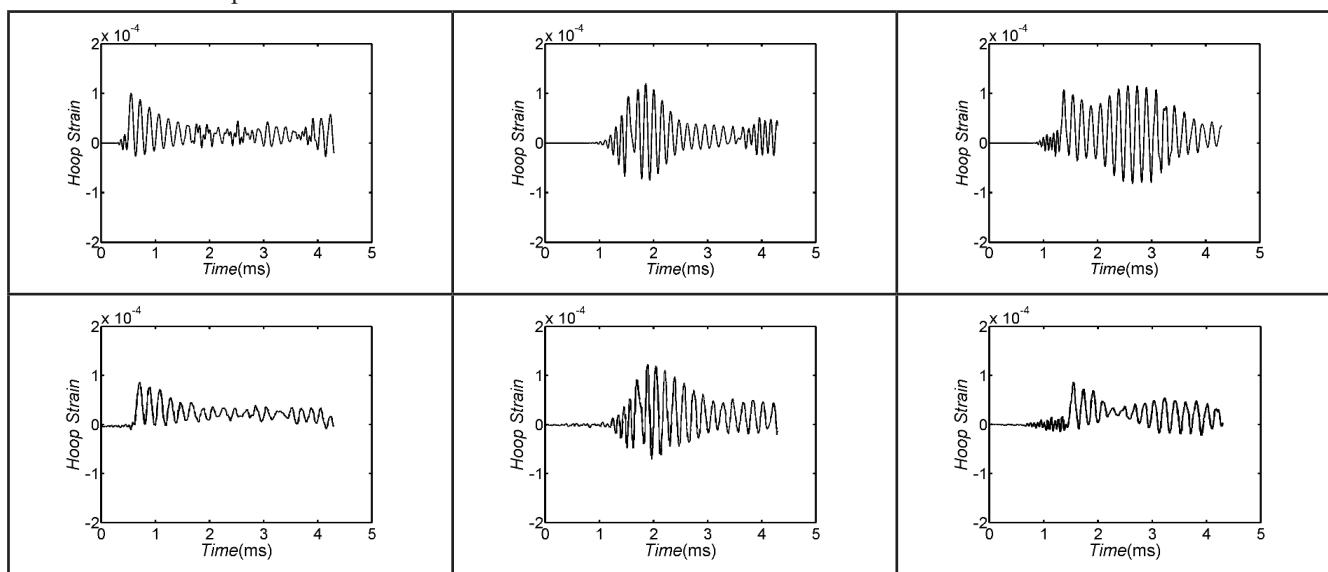


Fig. 1 Hoop strain for an experimental simply-supported tube under a detonation loading. Top row; analytical solution. Bottom row; experimental data [2]. Left column are for gauge 5, detonation velocity of 1699.7 m/s. Middle and right columns are for gauge 10, detonation velocities of 1478.8 and 1699.7 m/s, respectively.

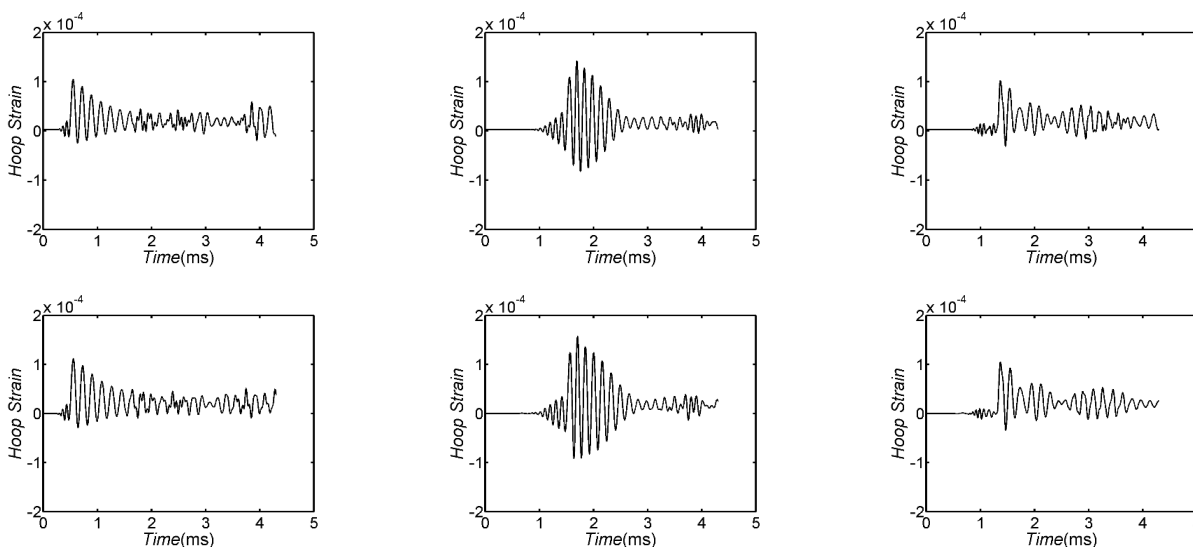


Fig. 2 Hoop strain for an experimental clamped-free tube under a detonation loading. Top row; analytical solution. Bottom row; FE results. Left column are for gauge 5, detonation velocity of 1699.7 m/s. Middle and right columns are for gauge 10, detonation velocities of 1478.8 and 1699.7 m/s, respectively

